

OPTIMUM HIGH IMPEDANCE SURFACE CONFIGURATION FOR MUTUAL COUPLING REDUCTION IN SMALL ANTENNA ARRAYS

N. Capet^{1,*}, C. Martel², J. Sokoloff³, and O. Pascal³

¹CNES, Antenna Department, 18 Avenue E. Belin, 31401 Toulouse cedex 9, France

²ONERA-DEMR, 2 Avenue E. Belin, BP 4025, Toulouse 31055, France

³Université de Toulouse UPS, INPT, CNRS LAPLACE (Laboratoire Plasma et Conversion d'Énergie), 118 Route de Narbonne, F-31062 Toulouse cedex 9, France

Abstract—In this paper, the electromagnetic properties of two different High Impedance Surfaces (HIS) with or without Electromagnetic Band Gap (EBG) in different configurations are investigated for mutual coupling reduction in small antenna arrays. The resonant mechanisms of these structures are studied using transmission calculations in a parallel plate waveguide. An optimum configuration is then proposed. It is shown that a good isolation performance can be achieved without the need of metallic vias when the structure is embedded in a metallic cavity, which limits significantly the number of HIS cells needed to perform a good isolation and the cost of manufacture.

1. INTRODUCTION

Mutual couplings in an array can represent severe drawbacks in some applications. In Controlled Reception Pattern Antenna (CRPA) applications, the antenna generally consists of an array of a few elements separated by a physical distance of about half a free space wavelength [1]. Therefore, mutual couplings between the elements of the array are generally strong and degrade the antenna and overall system performances [2]. Numerous strategies can be used to reduce mutual coupling in an array such as: corrugations [3, 4], Split Ring

Received 5 May 2011, Accepted 9 July 2011, Scheduled 20 July 2011

* Corresponding author: Nicolas Capet (nicolas.capet@cnes.fr).

Resonators (SRR) [5] and Defected Ground Structures (DGS) [6, 7]. Moreover, mushroom like High Impedance Surfaces (HIS) are well described in [8] and are well known to suppress surface waves and thus to improve the isolation of radiating elements in an array. This article focuses on such HIS technology and the way to optimize the insertion of the structure in a small array. Although the metamaterial unit cells of the HIS are very small compared to the wavelength, typically below $\lambda_0/10$, only a few rows of these structures can be inserted between the elements. Thus a trade-off between mutual coupling and the inter-element distance reduction has to be made.

Many different Electronic Band Structures based on mushroom like HIS as introduced in [8] have been designed and inserted between two antennas to reduce the coupling levels [9–13]. Generally, these structures consist of metallic patches printed on the substrate of the patch antennas and connected or not to the ground plane with a metallic vias. For single layer structures, the size of the patches is about half the substrate wavelength [11]. We can easily understand that this type of structure can not be used for CRPA applications due to the size of the unit cell. Thus, to optimize the compactness, a simple design of a two layered High Impedance Surface structure will be used inspired from [14], although further improvements in terms of size and cost can be achieved [15].

The use of metallic vias has been studied in our previous works [16, 17]. Their removal presents some advantages. Indeed, their manufacture is restrictive, especially regarding to the maximum thickness allowed by standard industrial processes. They are so expensive to build that their cost can represent a significant part of the total price of the antenna. Moreover, their radii can also lead to interesting discussions as the so called plasmonic resonance is related to this parameter [18, 19]. However, this topic is not developed in the present paper since our goal is to improve the isolation between radiating elements using a structure without vias.

In this paper, two high impedance surfaces are studied: one with metallic vias, the other without. Their capability to suppress surface waves has already been modeled and discussed in [20]. In the present paper, a conventional study of an infinite lattice of HIS cells is carried out leading to useful field distribution on an elementary cell. The resonant mechanisms of these structures with a limited number of cells are then studied in view of being integrated within an array. The way the structure is inserted is also assessed and highlights the impact of edge effects.

In Section 2, the designs of two square shaped HIS with or without metallic vias are presented together with their high impedance surface

properties. The dispersion properties of these structures highlight their differences.

In Section 3, an innovative means of characterizing the computed performances of the HIS for mutual coupling reduction is used (Figure 6) to study its frequency behavior. It is shown that the capability of the HIS with EBG is greatly affected by its size (i.e., the number of cells of the HIS has an impact on both the frequency stop bands and the attenuation levels) (Figures 7 and 8). Two different configurations are studied: when the HIS with EBG is embedded or not.

Finally, a study of the resonant processes is carried out in Section 4 for both structures (with and without vias) and both configurations (embedded or non embedded). It is shown that the use of the embedded configuration enables the excitation of the HIS resonance independently of the number of cells. As a consequence, this configuration enables an efficient mutual coupling reduction with a very limited number of cells. Moreover, it allows the suppression of the metallic vias — i.e., the use of HIS with no EBG — while keeping good isolation properties.

2. HIGH IMPEDANCE SURFACES

2.1. Design of Two Layered HIS

The need to improve CRPA performances in GNSS application is recurrent, especially regarding to the mutual coupling levels between the antenna elements [22]. Therefore, two HIS have been designed in the L frequency band. The HIS with metallic vias has been designed to operate at 1.36 GHz. The choice of a two layered structure has been made in [16] and its design is reminded in Figure 1. Indeed, the high impedance resonance is due to the combination of a capacitive and an inductive effect [8]. As the inductance is directly linked to the size of the cell and the thickness of the structure [23], it is not feasible to use high inductive effect while preserving a compact unit cell. Therefore, a structure providing a high left handed capacitance value has been considered. Finally the size of the unit cell edge is close to $\lambda_0/20$.

The first HIS cell design (Figure 1) consists of a two layer built dielectric substrate ($\epsilon_r = 2.2$) with a total thickness of 4.95 mm as shown in Figure 1. A high capacitance value is obtained with closely coupled patches, which are printed on both sides of a thin dielectric substrate (0.127 mm thickness). Square elements are used for the top and bottom patches, respectively. Vertical metallised vias connect the patches of the top layer to the ground plane in such a way as to create a left-handed inductive effect [14]. The second HIS design is identical to

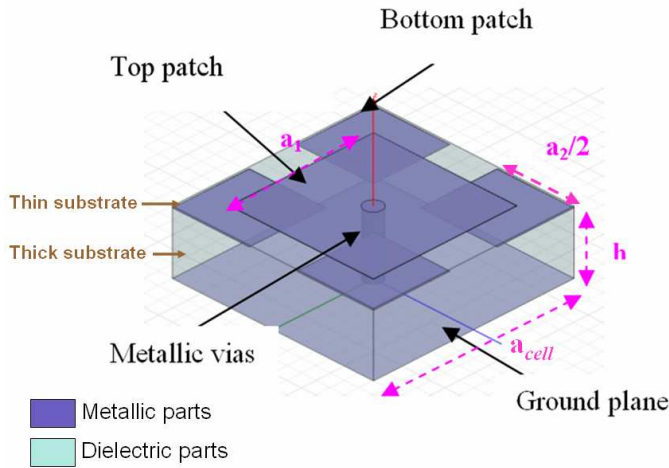


Figure 1. View in 3 dimensions of the HIS cell with metallic vias ($a_1 = 10$ mm, $a_2 = 5.35$ mm, $a_{cell} = 14$ mm, $h = 4.95$ mm).

the first one except that no vertical metallised vias connect the patches of the top layer to the ground plane. Square shaped patches have been chosen for convenience in the observation of the studied fields.

2.2. High Impedance Effect

The study conducted in [17] is here extended to a via free HIS to compare both configurations. At resonance, a HIS is characterised by a high value of surface impedance and a reflection phase of zero. Using the finite element solver HFSS from Ansoft, the impedance surface and reflection phase have been computed under normal incidence. Taking advantage of the symmetry of the problem, the impedance surface is obtained by applying two perfect magnetic conductors (PMC) and two perfect electric conductors (PEC) on the sides of a HIS cell (Figure 2). By deembedding the wave port impedance up to the top of the cell, the surface impedance and the phase of the reflection coefficient can be obtained (Figure 3).

At the resonant frequency ($f = f_{HIS}$), the H field in the substrate of both cells is intense and almost uniform (Figure 4(a)). The presence of the metallic vias does not play a major role for this resonance. That is why the HIS with or without metallic vias resonate at the same frequency. The E field is concentrated between the closely coupled square patches, where the capacitance value is high (Figure 4(b)).

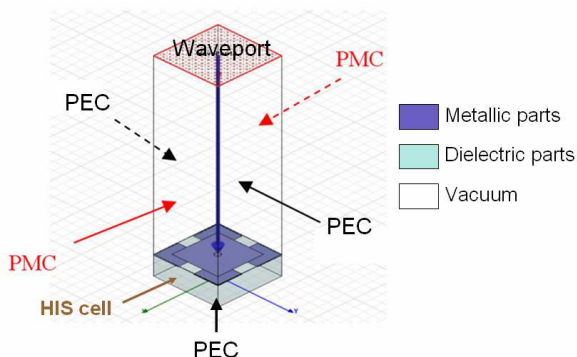


Figure 2. HIS cell with vias simulated with equivalent periodic boundary conditions under a normal incident wave.

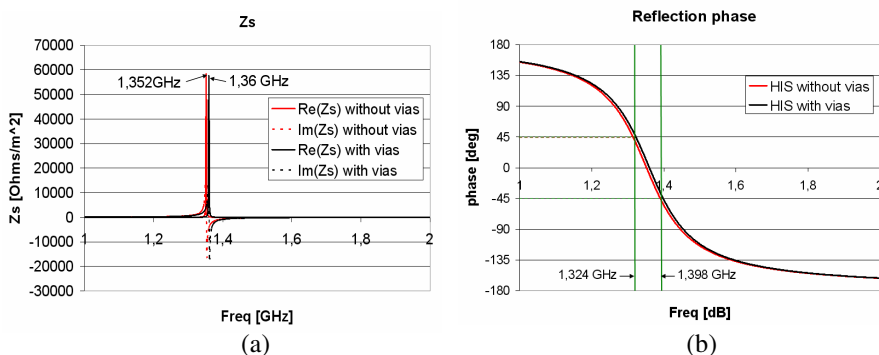


Figure 3. Simulation of an infinite plane of HIS with and without metallic vias under normal incidence: (a) real and imaginary part of the surface impedance, (b) reflection coefficient phase.

2.3. Dispersion Properties

As shown in Section 2.2, the two HIS designs cannot be differentiated by their surface impedance properties under normal incidence. In Figure 5, the dispersion properties of a plane constituted of infinitely periodic HIS cells — with or without vias — are depicted. Our interest will focus on the Γ - X direction of propagation [21]. This propagation direction is coherent with the ability of the structure to reduce mutual coupling in a linear array of thin patches in E plane polarisation.

It is observed in Figure 5 that the HIS without metallic vias does not present a band gap in this direction of propagation contrary to

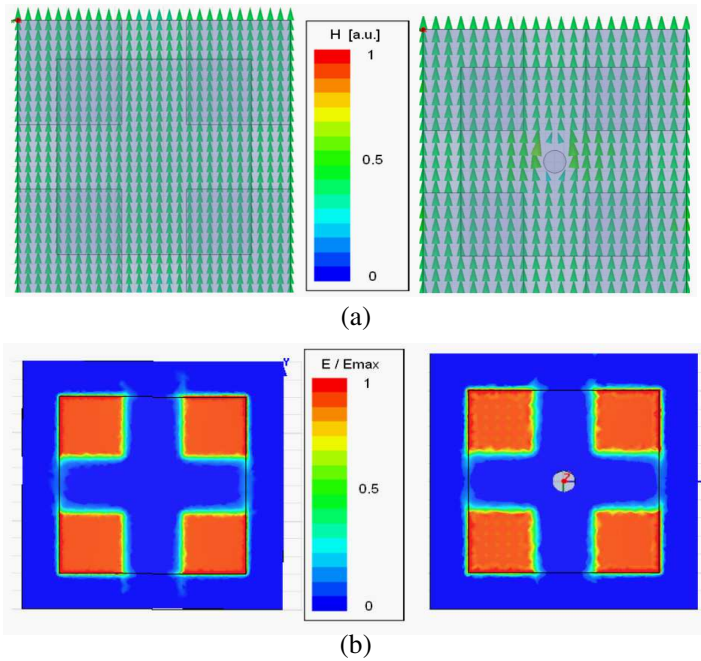


Figure 4. Field illustration at the respective HIS resonant frequency for the HIS without and with metallic vias respectively on the left and on the right, (a) H field vector between the bottom patch and the ground plane, (b) magnitude of the E field between the top and bottom square patches.

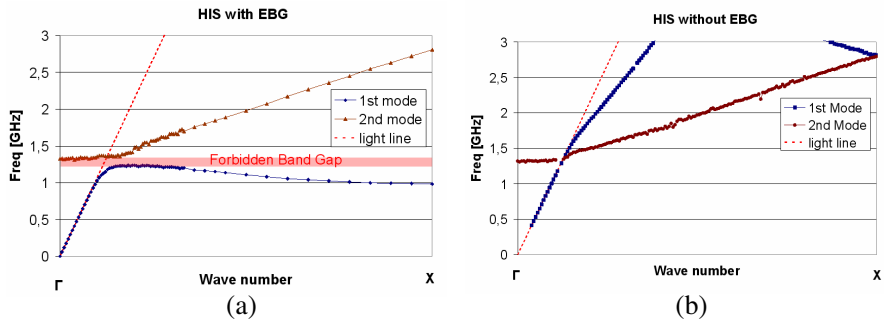


Figure 5. Band diagrams of the HIS (a) with metallic vias, (b) without metallic vias.

the HIS with metallic vias. Thus, the HIS without vias might not be able to stop surface currents propagation and reduce mutual coupling between antennas. It is consistent with [14, 20] and [23] and confirms that the first mode is disturbed by the presence of the vias, which induces the band gap — the inductive effect works as a low pass for the first mode. Thus, the computation of the band diagrams highlights the differences between the two structures.

3. PROPERTIES OF A FINITE HIS

3.1. Description of the Setup

In Section 2, we have computed some electromagnetic properties of an infinite plane constituted of periodic HIS cells. Since the space is limited between the radiating elements of the array, the EM properties of a few periods of both HIS structure is considered.

It has been shown that the HIS resonant frequency of such mushroom structures is slightly shifted depending on the angle of the incident wave [11]. Within a linear array of thin patches in E plane polarisation, it can be assumed that the coupling between the elements is in the form of grazing incidence. In view of characterising the properties of the HIS in these conditions, transmission measurements of a waveguide containing the two types of HIS are carried out. The following setup is valid as far as the coupling between the radiating elements is mainly due to TM_0 substrate modes, which is the case for thin patches or cavity backed patch antennas [24].

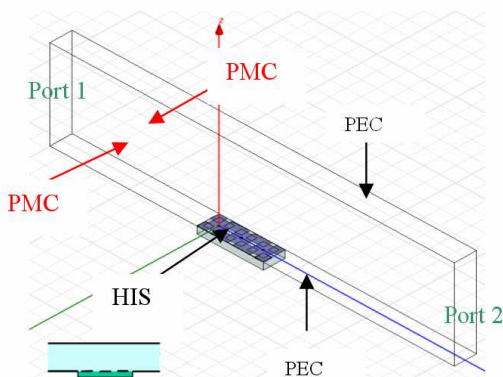


Figure 6. 3D illustration of the guide containing the HIS embedded structure.

The wave guide is composed of two perfect metallic plates on the top and the bottom. The HIS is inserted in the wave guide in two different ways: on or embedded in a metallic cavity connected to the bottom plate of the guide (as illustrated in Figure 6) — the embedded configuration is studied as it has the potential to isolate radiating elements more efficiently [16, 17]. The number of cells of the HIS can be adjusted. When the cells are not embedded, the ground of the cells corresponds to the bottom metallic part of the guide. The walls of the guide are composed of perfect magnetic conductors. Thus, a TEM mode can propagate in this guide.

This means of characterisation is relevant of the coupling phenomenon between two patch antennas. Indeed, for waves propagating from one microstrip antenna to another, the E field vector is predominantly normal to the ground plane surface and the H field is mainly contained in the plane orthogonal to the propagation direction and tangential to the ground plane.

3.2. Transmission Results

As shown in Figure 7, the wave guide containing the HIS with EBG (i.e., the HIS with metallic vias) exhibits stop bands at different frequencies, depending on the number of cells considered. From the study of the HIS resonance under normal incidence, it was expected that this resonance appeared in the guide around $f_{\text{HIS}} = 1.36$ GHz. It occurs when the HIS is embedded in the guide (Figure 7(b)), but it can not be observed for the not embedded HIS configuration with a limited number of cells (Figure 7(a)). It is also illustrated that the

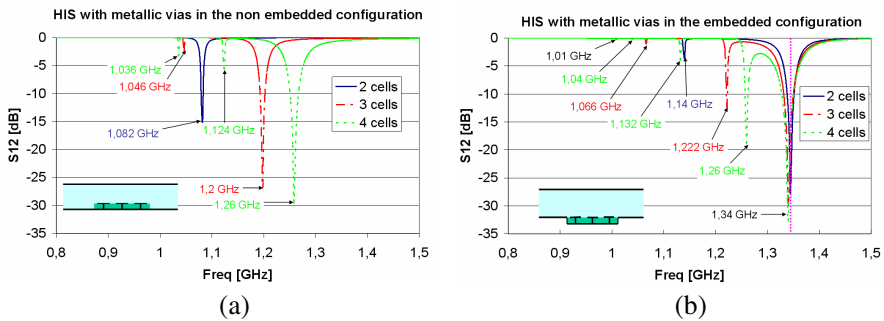


Figure 7. Transmission through a wave guide constituted of two metallic plates (top and bottom), two PMC walls and containing (a) the HIS with EBG not embedded, (b) the HIS with EBG embedded.

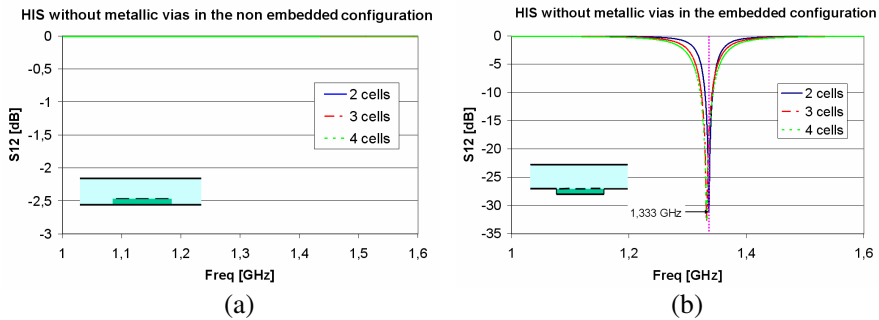


Figure 8. Transmission through a wave guide constituted of two metallic plates (top and bottom), two PMC walls and containing (a) the HIS without EBG non embedded, (b) the HIS without EBG embedded.

more inserted cells there are in the guide, the more resonant frequencies there are. The HIS excited under normal incidence does not provide all these additional resonances.

In Figure 8, the wave guide containing the HIS without EBG (i.e., the HIS without metallic vias) in the not embedded configuration does not exhibit stop bands. This confirms the results obtained in Figure 5 where no band gap appears in the dispersion curves. However, in the embedded configuration, a cut-off appears at the resonance frequency of the HIS. This resonance is independent of the number of cells. Finally, for both HIS in the embedded configuration, a resonance appears at the frequency of the HIS resonance. This phenomenon is of a major interest and represents the main contribution of this article. It is investigated in Section 4.2 where a physical interpretation is proposed to explain the origin of this resonance.

4. STUDY OF THE RESONANCES

In Section 3, two important results have been highlighted. On the one hand, depending on the number of cells considered, the HIS with EBG exhibits stop bands at different frequencies. On the other hand, for both HIS in the embedded configuration, a transmission cut off appears at the frequency of the HIS resonance independently of the number of cells inserted in the guide. In this section, the field distribution of the HIS is studied in order to understand the resonant mechanisms involved in these structures.

4.1. The Non HIS Resonances ($f \neq f_{\text{HIS}}$)

The wave guide containing the HIS with EBG (i.e., the HIS with metallic vias) exhibits stop bands at different frequencies, depending on the number of cells considered. In Figure 9, the H field distribution at some of non HIS resonant frequencies for the 3 cells HIS with EBG is depicted.

As expected from its frequency response, for resonant frequencies different from the HIS resonant frequency ($f \neq f_{\text{HIS}}$), the non embedded configuration does not exhibit the H field distribution at the HIS resonance in the presence of a limited number of cells (Figures 9(a) and 9(b)). It shows that the environmental conditions of the HIS do not allow this resonance obtained in the case of an infinite plane.

In addition, it can be seen from Figure 9 that the H field orientation is not the same in the three cells. It illustrates that a resonance can be generated by a group of cells and affected by the presence of the metallic cavity. It is the case for all resonances, except the HIS resonance discussed in the Section 4.2. This is further illustrated in Figure 7, where various resonances can be observed depending on the configuration and the number of cells considered. It also explains the increase in the number of resonances as more cells are introduced in the guide.

4.2. The HIS Resonances ($f = f_{\text{HIS}}$)

In this section, the field distributions of the 3 HIS cells structures embedded in the wave guide are studied at the HIS resonance.

In Figure 10, the H field in the substrate of a 3 cell HIS with or without EBG embedded is shown at the HIS resonance. We can notice that the H field distribution is uniform in the substrate of the HIS without EBG and all these three cells resonate in phase with the same H field orientation. In the case of the HIS with EBG, we can notice that the H field distributions of the cells are similar. However, a uniform attenuation can be observed from cell to cell in the direction of wave propagation. For both cases each cell then works as when it was infinitely periodised and normally illuminated (Figure 4) and the same transmission levels are observed at this frequency (Figures 7(b) and 8(b)). This explains why Figure 4(a) is almost in accordance with Figure 10. It can be observed that the same high impedance resonance and frequency are achieved whether the two HIS are excited under normal or grazing incidence, independently of the number of cells considered. The edge effects introduced by the cavity containing the HIS recreate the necessary conditions for the apparition of the HIS resonance. Indeed, due to the shape of the HIS resonant mode, the

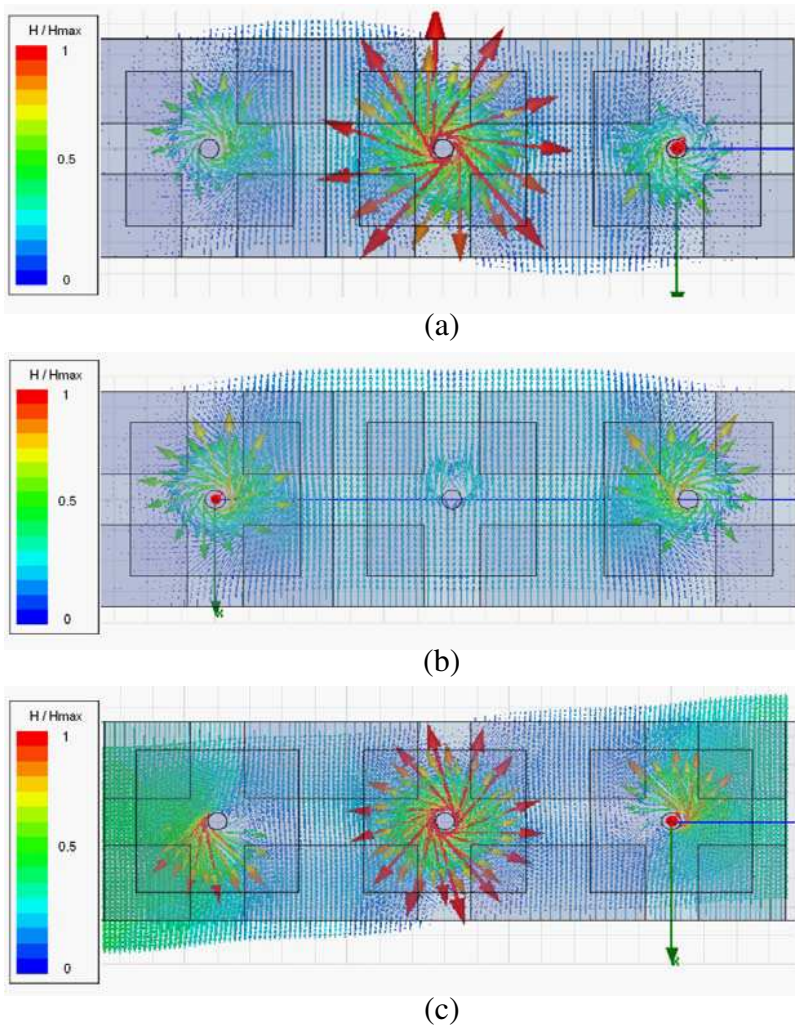


Figure 9. H field distribution in the substrate of the 3 cells HIS with EBG. (a) Non embedded configuration at 1.046 GHz. (b) Non embedded configuration at 1.2 GHz. (c) Embedded configuration at 1.22 GHz.

metallic walls of the cavity containing the HIS works as a symmetry plane. The HIS resonant mode existing in the case of an infinite plane constituted of HIS cells can be now excited in the presence of a very limited number of cells.

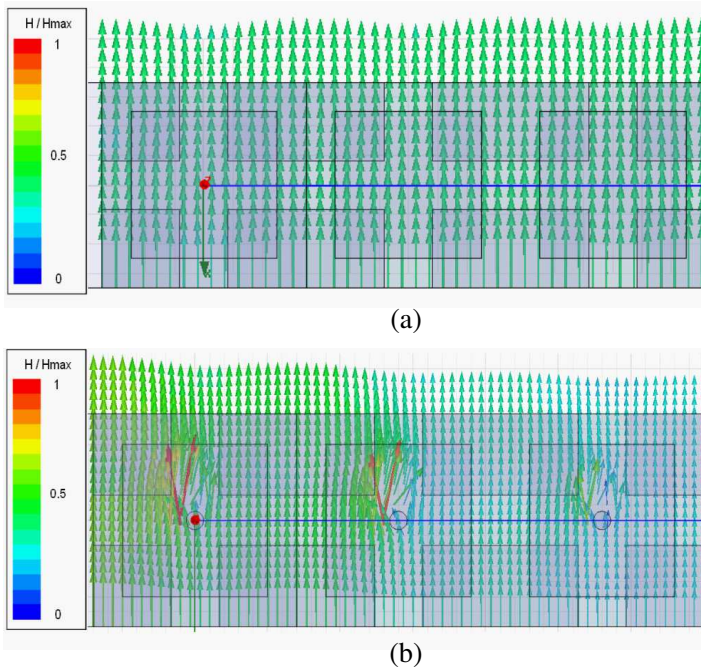


Figure 10. H field in the substrate of a 3 cell HIS in the embedded configuration. (a) Embedded configuration without vias (1.33 GHz). (b) Embedded configuration with vias (1.34 GHz).

5. CONCLUSION

In this paper, the properties of two HIS structures have been investigated, one with EBG and the other without. These structures are composed of several cells for mutual coupling reduction between L band patch antennas for CRPA application. An innovative characterisation method, based on waveguide transmission simulations, has been used to assess the decoupling properties of the HIS under grazing incidence with a limited number of cells.

Two different HIS design configurations — the embedded and non embedded HIS — have been studied. It has been shown that depending on the number of cells considered, the HIS with EBG exhibits stop bands at different frequencies. Moreover, for both HIS in the embedded configuration, a transmission cut off appears at the frequency of the HIS resonance independently of the number of cells inserted in the guide.

The study of the resonant mechanisms has shown that most of the

resonances are based on multiple cells. This explains the frequency dependence regarding the number of cells considered. However, in the embedded configuration, the side effects introduced by the cavity containing the HIS recreate the necessary conditions for the apparition of the HIS resonance. This explains why this resonance appears independently of the number of the cells.

In conclusion, it has been shown that the HIS structure in the embedded configuration provides the optimum performance for our application. It allows the use of a very limited number of cells while preserving a good isolation. It can also be noticed that the HIS with metallic vias allows multi-frequency isolation. Moreover, the design does not require metallic vias, which limits significantly the cost of manufacture.

As shown in this paper with a basic HIS cell and considering the diversity of possible HIS topologies, similar studies could be done with other kind of unit cells. Complementary experimental works will be performed to confirm the promising simulation results of this paper.

ACKNOWLEDGMENT

N. Capet wishes to acknowledge ONERA (The French Aerospace Lab) for providing the funding and the place for this work during his Ph. Doctor courses.

REFERENCES

1. Van Trees, H. L., *Optimum Array Processing, Part IV of Detection, Estimation, and Modulation Theory*, Wiley-Interscience, 2002.
2. Ngai, E. C. and D. J. Blejer, "Mutual coupling analyses for small GPS adaptive arrays," *IEEE Antennas and Propagation Society International Symposium*, Vol. 4, 3841, 2001.
3. Kildal, P.-S., "Artificially soft and hard surfaces in electromagnetics and their application to antenna design," *23rd European Microwave Conference*, 30–33, Sep. 6–10, 1993.
4. Rajo-Iglesias, E., O. Quevedo-Teruel, and L. Inclan-Sanchez, "Planar soft surfaces and their application to mutual coupling reduction," *IEEE Transactions on Antennas and Propagation*, Vol. 57, No. 12, 3852–3859, Dec. 2009.
5. Buell, K., H. Mosallaei, and K. Sarabandi, "Electromagnetic metamaterial insulator to eliminate substrate surface waves,"

- IEEE Antennas and Propagation Society International Symposium*, Vol. 2A, 574–577, Jul. 3–8, 2005.
6. Guha, D., S. Biswas, M. Biswas, J. Y. Siddiqui, and Y. M. M. Antar, “Concentric ring-shaped defected ground structures for microstrip applications,” *IEEE Antennas and Wireless Propagation Letters*, Vol. 5, No. 1, 402–405, Dec. 2006.
 7. Chiu, C.-Y., C.-H. Cheng, R. D. Murch, and C. R. Rowell, “Reduction of mutual coupling between closely-packed antenna elements,” *IEEE Transactions on Antennas and Propagation*, Vol. 55, No. 6, 1732–1738, Jun. 2007.
 8. Sievenpiper, D., L. Zhang, R. F. J. Broas, N. G. Alexopolous, and E. Yablonovitch, “High impedance electromagnetic surfaces with a forbidden frequency band,” *IEEE Transactions on Microwave Theory and Techniques*, Vol. 47, No. 11, Nov. 1999.
 9. Yang, F. and Y. Rahmat-Samii, “Microstrip antennas integrated with electromagnetic band-gap (EBG) structures: A low mutual coupling design for array applications,” *IEEE Transactions on Antennas and Propagation*, Vol. 51, No. 10, 2936–2946, Oct. 2003.
 10. Simovski, C. R. and A. A. Sochava, “High-impedance surfaces based on self-resonant grids. Analytical modelling and numerical simulations,” *Progress In Electromagnetics Research*, Vol. 43, 239–256, 2003.
 11. E. Rajo-Iglesias, O. Quevedo-Teruel, and L. Inclan-Sanchez, “Mutual coupling reduction in patch antenna arrays by using a planar EBG structure and a multilayer dielectric substrate,” *IEEE Transactions on Antennas and Propagation*, Vol. 56, No. 6, 1648–1655, Jun. 2008.
 12. Fan, M. Y., R. Hu, Z. H. Feng, X. X. Zhang, and Q. Hao, “Advance in 2D-EBG research,” *Journal of Infrared Millimeter Waves*, Vol. 22, No. 2, 2003.
 13. Lin, B.-Q., Q.-R. Zheng, and N.-C. Yuan, “A novel spiral high impedance surface structure for size reduction,” *Microwave and Optical Technology Letters*, Vol. 49, No. 9, Sep. 2007.
 14. Caloz, C. and T. Itoh, *Electromagnetic Metamaterials: Transmission Line Theory and Microwave Applications: The Engineering Approach*, Wiley-Interscience, 2006.
 15. Costa, F., S. Genovesi, and A. Monorchio, “On the bandwidth of high-impedance frequency selective surfaces,” *IEEE Antennas and Wireless Propagation Letters*, Vol. 8, 1341–1344, 2009.
 16. Capet, N., C. Martel, J. Sokoloff, and O. Pascal, “Reduction of the mutual coupling between two adjacent patches using various

- ideal High Impedance Surface positionings,” *Proceedings of the 3rd European Conference on Antennas and Propagation, EuCAP 2009*, 3151–3154, Mar. 23–27, 2009.
17. Capet, N., C. Martel, J. Sokoloff, and O. Pascal, “Study of the behaviour of a two layered high impedance surface with electromagnetic band gap,” *Proceedings of the Fourth European Conference on Antennas and Propagation, EuCAP 2010*, 1–4, Apr. 12–16, 2010.
 18. Luukkonen, O., M. G. Silveirinha, A. B. Yakovlev, C. R. Simovski, I. S. Nefedov, and S. A. Tretyakov, “Effects of spatial dispersion on reflection from mushroom-type artificial impedance surfaces,” *IEEE Transactions on Microwave Theory and Techniques*, Vol. 57, No. 11, 2692–2699, Nov. 2009.
 19. Luukkonen, O., F. Costa, C. R. Simovski, A. Monorchio, and S. A. Tretyakov, “A thin electromagnetic absorber for wide incidence angles and both polarizations,” *IEEE Transactions on Antennas and Propagation*, Vol. 57, No. 10, 3119–3125, Oct. 2009.
 20. Luukkonen, O., A. B. Yakovlev, C. R. Simovski, and S. A. Tretyakov, “Comparative study of surface waves on high-impedance surfaces with and without vias,” *IEEE Antennas and Propagation Society International Symposium*, 1–4, Jul. 5–11, 2008.
 21. Joannopoulos, J. D., S. G. Johnson, J. N. Winn, and R. D. Meade, *Photonic Crystals: Molding the Flow of Light*, 2nd edition, Princeton University Press, 2008.
 22. Ngai, E. C. and D. J. Blejer, “Mutual coupling analyses for small GPS adaptive arrays,” MIT Lincoln Laboratory, 2001.
 23. Rahmat-Samii, Y., “EBG structures for low profile antenna designs: What have we learned?,” *Proceedings of the Second European Conference on Antennas and Propagation, EuCAP 2007*, 1–5, Nov. 11–16, 2007.
 24. Pozar, D., “Considerations for millimeter wave printed antennas,” *IEEE Transactions on Antennas and Propagation*, Vol. 31, No. 5, 740–747, Sep. 1983.